

## Crossing the great divide between single crystal reactivity and catalytic selectivity with pressure transients

Christian Reece<sup>1</sup>, Evgeniy Redekop,<sup>2</sup> Stavros Karakalos,<sup>3</sup> Cynthia M. Friend<sup>1</sup> and Robert. J. Madix<sup>4\*</sup>

1. Harvard University, Department of Chemistry and Chemical Biology, Cambridge, MA, USA
2. University of Oslo, Department of Chemistry, Centre for Materials Science and Nanotechnology (SMN), Oslo, Norway
3. University of South Carolina, College of Engineering and Computing, Columbia, SC, USA
4. Harvard University, School of Engineering and Applied Science, Cambridge, MA, USA

\*corresponding author: [rmadix@seas.harvard.edu](mailto:rmadix@seas.harvard.edu)

**Quantitative prediction of selectivity for catalytic reactions is essential to the design of efficient catalytic processes and requires detailed knowledge of reaction mechanism and rate constants. This first-of-a-kind study accurately predicts the product distribution resulting from the complex reaction network governing oxidative coupling of methanol catalysed by nanoporous Au between 360 - 425 K and for a vast range of pressures using the kinetics and mechanism derived from fundamental studies on single-crystal Au. Analysis of transient product responses to micropulses of methanol over nanoporous gold yield precise understanding of the marked dependence of selectivity on pressure, surface oxygen coverage and temperature. The key to high selectivity for methyl formate is the surface lifetime and abundance of methoxy. This successful microkinetic modeling of catalytic reactions across a wide set of reaction conditions is broadly applicable to predicting catalytic selectivity and provides a pathway to designing more efficient catalytic processes.**

### Introduction

Rational design of new catalyst materials and catalytic processes is a scientific “holy grail” with the potential of greatly improving the efficiency of chemical production through increasing the selectivity for desired products. Recently, a massive effort has been launched to design materials, including catalysts, with specific and predictable functions.<sup>1,2</sup> This effort has largely been theory-based and has focused on the development of “descriptors” that predict catalyst *activity* through calculation of thermodynamic properties.<sup>3,4</sup> One of the major challenges in catalysis, however, is catalytic behavior—especially, selectivity—which is controlled by kinetics, requiring fundamental information about rate constants, rate laws and time-scales for possible restructuring of catalytic material under different reaction conditions.

Historically, catalytic processes were developed by empirical screening of materials. Rates and selectivities for specific reactions were measured as a function of reactant partial pressure and temperature,<sup>5</sup> the elementary steps often inferred, providing a means for interpolating reactor performance over restricted ranges of temperature and reactant pressures. Determination of accurate rate constants and reaction sequences that can be used for extrapolation to a wider range of conditions was generally beyond the scope of such research, and, hence, the empirical modeling is only reliable for a narrow range of conditions and for specific catalyst materials.

While the empirical approach was effective in early catalyst development, the invention of new processes requires a systematic and informed approach. Modern surface science tools have enabled the dissection of complex reactions into molecular-scale elementary steps and provided the associated rate constants for well-defined conditions, *at first inspection*, at very low-pressure. A major goal is to employ accurately measured rate parameters, obtained from such model studies, to predict and understand the performance of heterogeneous catalysts under operational conditions. At the root of this translation across orders of magnitude of pressure and over a wide range of temperature (hundreds of degrees Kelvin), and from a well defined surface to the actual catalyst is the application of fundamental understanding of the kinetics and the response of the surface to the changes in reaction conditions. These differences in conditions have been previously referred to as the *pressure and material gaps* (often neglecting critical temperature differences), but they actually comprise a *knowledge continuum*, which can be understood from basic principles.

Overall, the challenge is to scale the model studies from one set of conditions with specific adsorbate coverages, temperature and material to catalytic conditions. The higher temperatures used during catalysis may maintain a relatively low concentration of reaction intermediates, often paralleling lower pressure model conditions. Elevated temperatures in catalytic reactors also change the surface lifetimes of adsorbates and the rates of specific elementary steps and further may lead to important changes in materials structure compared to the model studies. Altogether, these complexities render translation of catalytic behavior across these vastly different conditions challenging.

Herein, we have used transient pulse-response kinetic measurements under Knudsen flow conditions – Temporal Analysis of Products (TAP)<sup>6</sup> – to provide a bridge between fundamental single crystal measurements and reactor performance at atmospheric pressure for selective oxidation of methanol by Au. Selective oxidation is an important subset of catalytic transformations that yields valuable products in the chemical and pharmaceutical industries.<sup>7-9</sup> *The reaction kinetics were monitored with millisecond time-resolution on the actual high-surface area catalyst material (nanoporous Ag<sub>0.03</sub>Au<sub>0.97</sub>) at the operational temperature.* Using the elementary steps, activation energies and pre-exponential factors determined from single crystal studies, we accurately predict the selectivity for the catalytic oxidative coupling of methanol to methyl formate over nanoporous gold catalysts under catalytic conditions. The approach used is general and applicable to many other catalytic reactions. The results show that the selectivity for ester formation depends on both temperature and pressure. We document and explain a significant “pressure” effect that arises from changes in the relative concentration of adsorbed reactive intermediates.

This work provides a new paradigm for quantitatively predicting catalytic behavior with broad applicability, even for multi-step and complex transformations. This paradigm holds the promise for delivering on “catalysis by design,” because understanding of the temperature and pressure effects on selectivity can be used to test the sensitivity of key steps to the composition and structure of catalyst materials as a function of reaction conditions, leading to the possibility of catalyst modification that targets the rates of specific elementary steps in the catalytic cycle.

## Results

### Reaction mechanism from studies in ultrahigh vacuum

Previous model studies<sup>10-12</sup> in ultrahigh vacuum have established the cycle for oxygen-assisted methanol esterification over metallic gold (Figure 1).

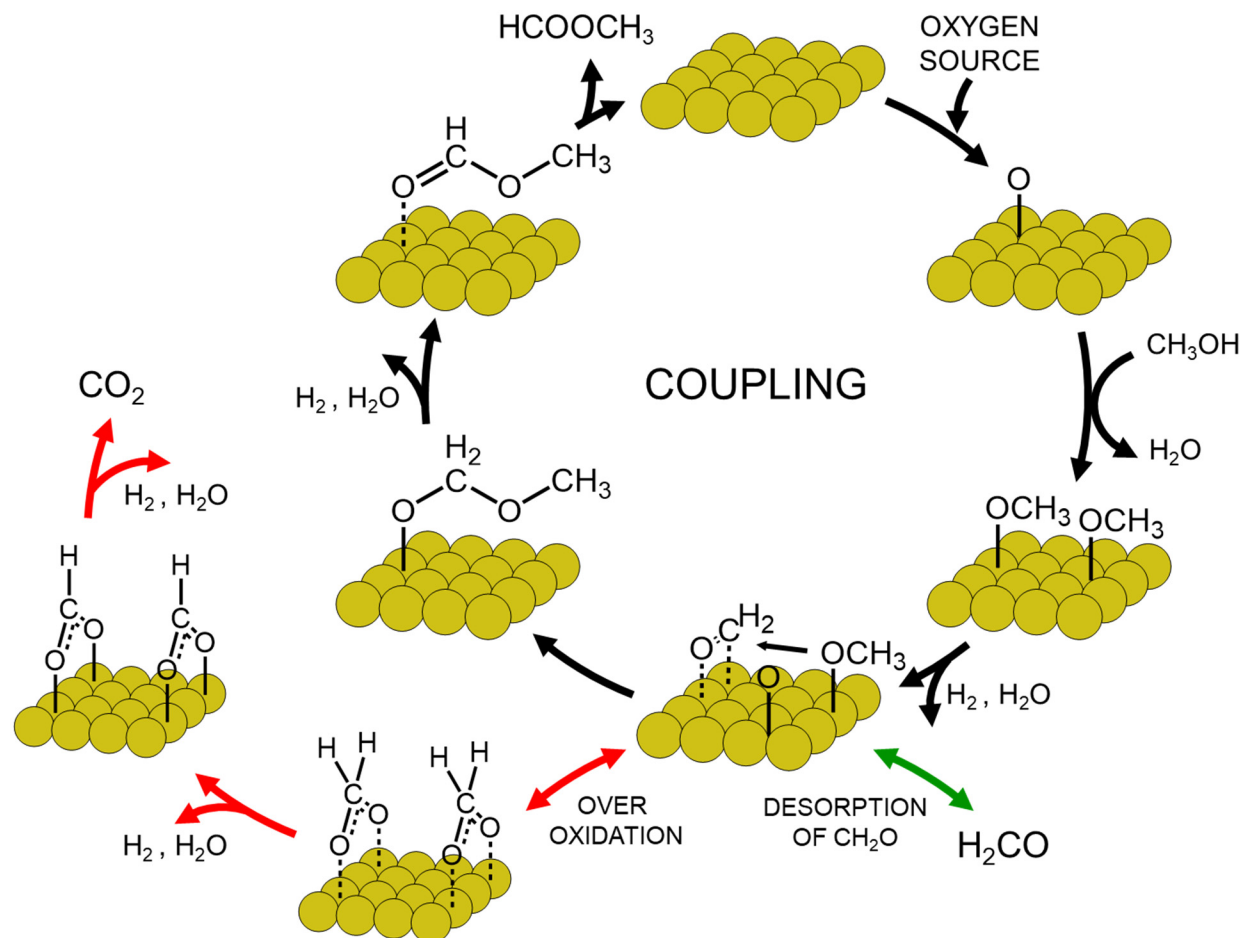


**Figure 1.** Elementary reaction steps for the oxidation of methanol on Au(111) containing O atoms on the surface, showing competing coupling and combustion.<sup>13–16</sup> Methanol is activated via atomic oxygen forming surface bound methoxy. The methoxy then undergoes  $\beta$ -H elimination to form surface-bound formaldehyde. Ester production occurs via nucleophilic attack of formaldehyde by unreacted methoxy and subsequent loss of H. Combustion is initiated through reaction of formaldehyde with O on the surface; formate, which yields CO<sub>2</sub>, is formed by loss of hydrogen to the surface. Water is a major byproduct of both pathways. The same pathway is observed on Au(110).

Adsorbed O initiates the catalytic cycle by selectively activating the CH<sub>3</sub>O-H bond to form adsorbed methoxy, which undergoes competing oxidative coupling to methyl formate or total combustion to CO<sub>2</sub>.<sup>13,14</sup> Temperature programmed reaction spectroscopy experiments (see Methods, Supplemental III) performed on the single crystal surface showed that the selectivity for ester formation depends strongly on the initial O coverage, ranging from nearly 100 % for 0.05 monolayers of O (Figure 2) to 20% at 0.50 monolayers.<sup>15</sup> The reactivity is essentially the same on Au(111) and Au(110) under these conditions. The mechanism of Scheme 1 contains all the elementary steps known to be involved in the oxygen-assisted coupling of methanol on gold.<sup>14–17</sup>

Remarkably, the mechanism derived from single-crystal studies predicts the general patterns of the *catalytic*, oxygen-assisted coupling of alcohols to esters in both the *gas and liquid phases* at atmospheric pressure and above.<sup>18</sup> Critical to the *catalytic* pathway is the formation of the adsorbed

O species, since pure metallic gold does not activate dioxygen at a measurable rate.<sup>19,20</sup> Nanoporous  $Ag_{0.03}Au_{0.97}$  is an excellent catalyst for selective methanol coupling,<sup>18,21,22</sup> the small amount of Ag facilitates  $O_2$  dissociation. Methanol and  $O_2$  partial pressures are selected to create the active O atoms, while preventing the formation of silver oxides<sup>23,24,25</sup>. The active site density on this catalyst is dictated by the low concentration of Ag at the surface and is between 0.02 and 0.05 ML. Indeed, the selectivity for methyl formate production from methanol and  $O_2$  is > 95% under steady state flow conditions at 1 atm;  $CO_2$  is the only other product.<sup>18,25</sup>

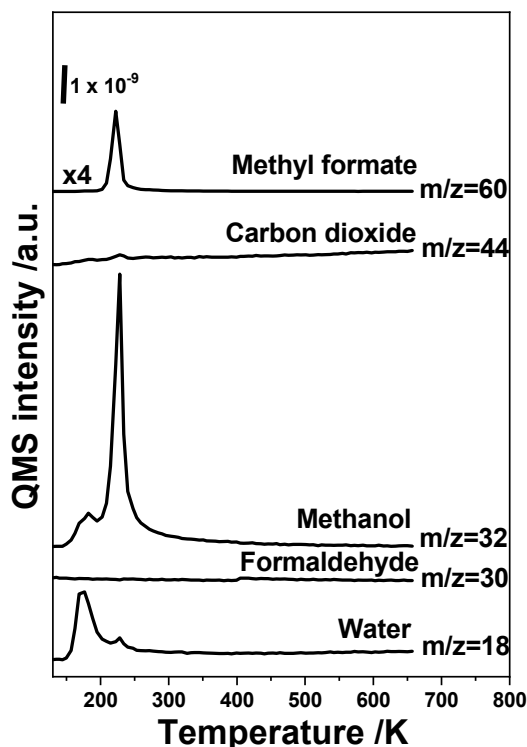
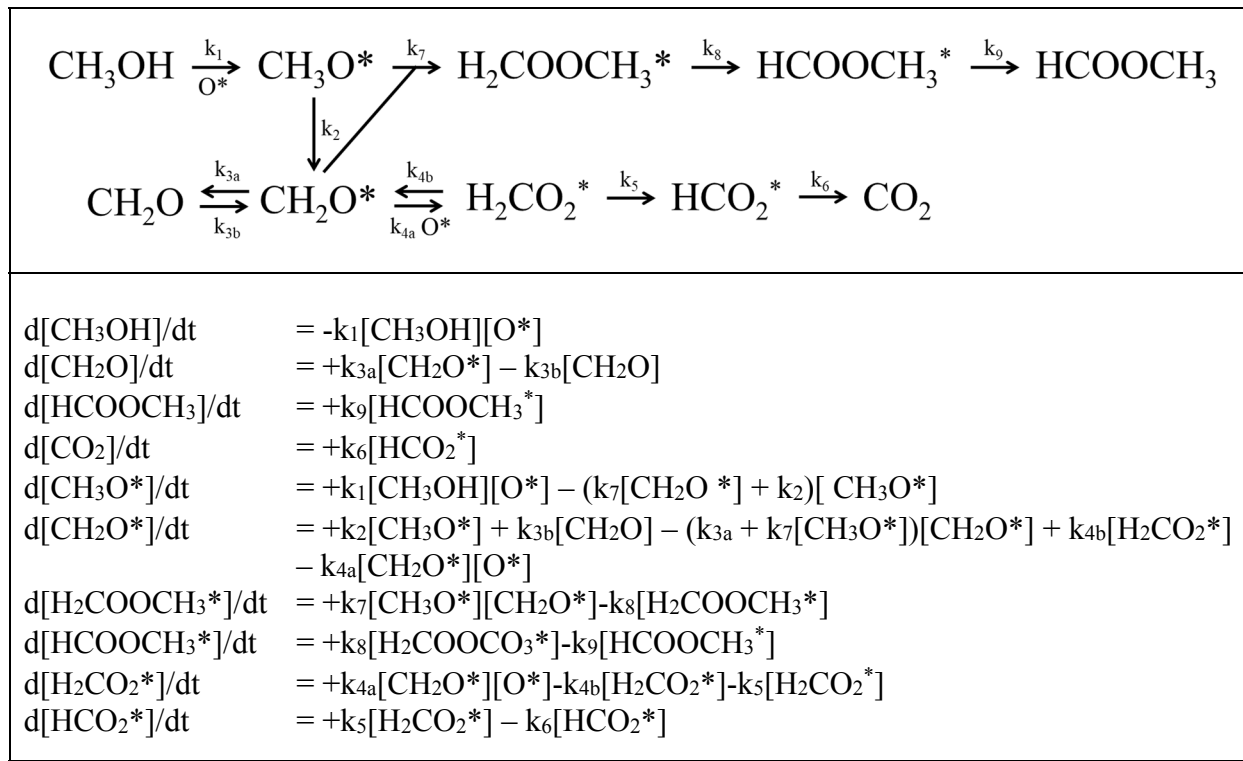


**Figure 2.** The temperature programmed reaction product spectrum resulting from the adsorption of methanol onto 0.05 ML of adsorbed O on Au(110) at 120 K followed by linear heating of the crystal. Nearly 100 % selectivity to oxygen-assisted coupling to methyl formate was observed.

### Formulating the reaction scheme

The *catalytic* cycle and its reactions used in our analysis are summarized by the network in Scheme I. In general, at the higher temperatures and pressures used under catalytic conditions, formaldehyde can desorb from the surface—a notable difference from the single crystal studies, which are conducted at such low temperatures that formaldehyde reacts before leaving the surface. In general, the low active site density of the catalyst and the relatively high operating temperature keeps the concentration of the reactive intermediates low, eliminating the potential effects of lateral interactions on the rate constants.



**Scheme I.** Summary of the reaction network in Figure 1 for methanol self-coupling over npAu catalyst with the elementary reaction rate expressions governing each species in the cycle used in the pulse experiment simulation; \*denotes a surface-bound species. Neither H<sub>2</sub> or H<sub>2</sub>O production is included in the network as they do not affect the relative selectivity for carbon containing products, and they are difficult to quantify experimentally. Nor do they effect the rates of any of the elementary steps.

### Effect of temperature and O coverage on selectivity on *noAu*

Catalysts of *nanoporous Ag<sub>0.03</sub>Au<sub>0.97</sub>* contained in a quartz reactor were preloaded with 0.015 ML of adsorbed O by exposure to O<sub>3</sub> using a pretreatment protocol that is known to favor selective formation of methyl formate from methanol.<sup>25</sup> The catalyst was then exposed to successive pulses of methanol diluted in argon, each pulse sufficiently small that (i) the transport of gas through the reactor was dominated by Knudsen flow, and (ii) reaction with *each* pulse produced insignificant change of the O surface concentration. *Multiple successive pulses of methanol lead to a gradual decline in the surface O coverage, allowing the O coverage to be controlled.* Product yields were determined by integration of mass spectrometric signals of each transient response (Supplementary I-II). The activity and selectivity of the catalyst was thus probed as a function of the O concentration and the temperature. Temperatures were chosen to span those most effective for the catalyst under steady flow conditions at atmospheric pressure.<sup>18,25</sup>

The product distribution strongly depends on both the O coverage and the temperature (Figure 3, solid points). At 423 K the conversion of the methanol pulse was initially 67 %, decreasing to zero as the surface O was consumed. Under these conditions, the dominant product was formaldehyde, unlike *either* the model studies in single crystal gold or the reactor studies; a significant amount of CO<sub>2</sub> and minor amounts of methyl formate were also produced. The amount of methyl formate produced increased as the temperature was decreased until at 363 K, it became the dominant product at the higher oxygen coverages (Figure 3). *Mass balances obtained via quantitative mass spectrometry account for all carbon containing products from methanol oxidation.*

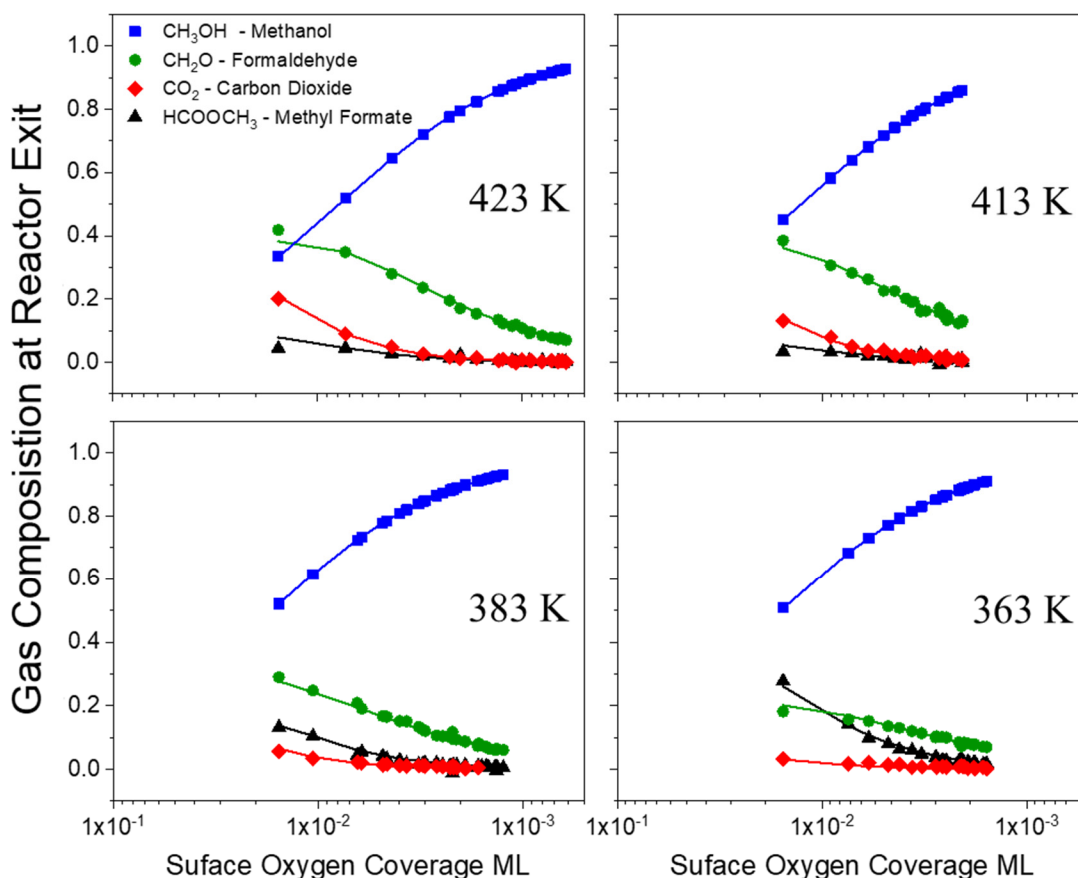


**Figure 3.** Gas composition at the reactor exit resulting from pulsed methanol exposure to *nanoporous Ag<sub>0.03</sub>Au<sub>0.97</sub>* at varying coverages of atomic oxygen and at different temperatures: solid points are from the pulse experiments; the solid lines are derived from the kinetic analysis using the network in Scheme 1. Oxygen coverages were determined from the cumulative amount of methanol reacted. (See Methods, Supplementary I-VI)

The predominance of formaldehyde production is different from both steady-state flow reactor experiments<sup>18</sup> on the same catalyst and the single crystal studies (Figure 2). As shown below, these pulse experiments provide a bridge between the vast pressure and temperature differences in these experiments that further validates the mechanism and reaction network (Figure 1, Scheme 1). One

critical link between these vastly different conditions is that at the temperature of these transient experiments (363 – 423 K ) desorption and readsorption of formaldehyde clearly occurs. Notably, formaldehyde, methyl formate and CO<sub>2</sub> appear sequentially in response to the methanol pulses (Figure 4), further indicating that the catalytic sequence determined using gold single crystals<sup>15</sup> also applies the nanoporous Ag<sub>0.03</sub>Au<sub>0.97</sub> catalyst at reactor temperature. Use of rate constants obtained from the model studies could then be used as the basis to quantitatively model the product yields (Figure 3) obtained from the transient responses (Figure 4), providing a quantitative link between the various sets of conditions.

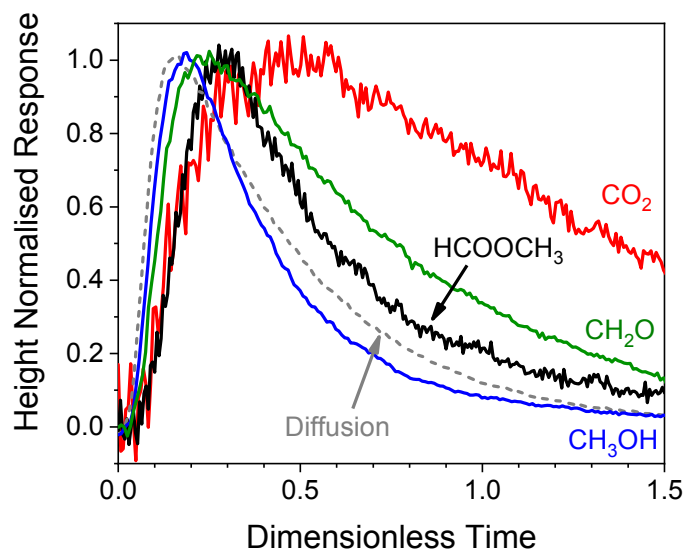


**Figure 4.** Height-normalized transient responses measured for methanol, formaldehyde, methyl formate and carbon dioxide after exposure of O-covered nanoporous Ag<sub>0.03</sub>Au<sub>0.97</sub> to a pulse of methanol demonstrates the differences in the time-responses for the various species. The progression of the product peaks to higher times in the order of formaldehyde, methyl formate and carbon dioxide is indicative of the sequential nature of the catalytic cycle illustrated in Figure 1. The response of the inert marker (Ar) in the grey dashed line represents diffusional transport. In the experiment the temperature was 423 K and the O coverage was 0.0073 ML.

#### Determination of rate constants from fundamental studies.

Values for the kinetic parameters (A and E<sub>a</sub>, Table 1) for each elementary step in the mechanism were obtained by one of several methods (Supplementary III). For example, in steps involving C-H bond cleavage (k<sub>2</sub>, k<sub>4b</sub>, k<sub>5</sub>, k<sub>6</sub>, and k<sub>8</sub>), the pre-exponent and activation energy were determined experimentally by temperature programmed reaction (Methods) on single crystal gold (e.g. Figure 2). The rate-limiting step for methyl formate formation is C-H bond cleavage in the adsorbed methoxy,<sup>15</sup> so the kinetics of methyl formate evolution from the surface directly reflect k<sub>2</sub><sup>15</sup> (Table 1, Figure 2).<sup>26,27</sup> The values of the rate constant parameters determined for all steps are summarized in Table 1.

**Table 1.** Elementary reaction steps involved in the oxidative coupling of methanol and their respective values calculated from single crystal studies (Low Pressure) and the responses to the

methanol pulses (Pulse Exps.). The kinetic parameters calculated from the pulses were evaluated using Arrhenius plots of the rate constants taken from the regressed simulated pulse experiment within the limited temperature range accessible (373, 393, 413, and 423 K) using the values obtained from the model studies as a starting point.

Step			Pre-Exponent		Units	Activation Energy kJ/mol		R <sup>2</sup>	
			Low Pressure	Pulse Exp.		Low Pressure	Pulse Exp.		
k <sub>1</sub>	CH <sub>3</sub> OH + O*	→	CH <sub>3</sub> O* + OH*	2.83x10 <sup>-14</sup>	-	cm <sup>3</sup> /s	17.00	-	-
	CH <sub>3</sub> OH + OH*	→	CH <sub>3</sub> O* + H <sub>2</sub> O*						
k <sub>2</sub>	CH <sub>3</sub> O*	→	CH <sub>2</sub> O* + H	5.79x10 <sup>14</sup>	1.23x10 <sup>15</sup>	s <sup>-1</sup>	65.27	67.83	0.9965
k <sub>3a</sub>	CH <sub>2</sub> O*	⇌	CH <sub>2</sub> O	3.02x10 <sup>15</sup>	3.03x10 <sup>16</sup>	s <sup>-1</sup>	45.75	40.74	0.9680
k <sub>3b</sub>				0.90 <sup>†</sup>	0.25 <sup>†</sup>	-	-	-	0.8973 <sup>‡</sup>
k <sub>4a</sub>	CH <sub>2</sub> O* + O*	⇌	H <sub>2</sub> CO <sub>2</sub> *	1.00x10 <sup>-2</sup>	1.95x10 <sup>-2</sup>	cm <sup>2</sup> /s	16.87	34.60	0.9973
k <sub>4b</sub>				5.79x10 <sup>14</sup>	1.44x10 <sup>14</sup>	s <sup>-1</sup>	50.00	38.89	0.9761
k <sub>5</sub>	H <sub>2</sub> CO <sub>2</sub> *	→	HCO <sub>2</sub> * + H*	5.79x10 <sup>14</sup>	4.45x10 <sup>13</sup>	s <sup>-1</sup>	56.73	52.46	0.9999
k <sub>6</sub>	HCO <sub>2</sub> *	→	CO <sub>2</sub> + H*	5.79x10 <sup>14</sup>	-	s <sup>-1</sup>	95.82	-	-
k <sub>7</sub>	CH <sub>2</sub> O* + CH <sub>3</sub> O*	→	H <sub>2</sub> COOCH <sub>3</sub> *	1.00x10 <sup>-2*</sup>	3.11x10 <sup>-2</sup>	cm <sup>2</sup> /s	(5.00)**	19.56	0.9963
k <sub>8</sub>	H <sub>2</sub> COOCH <sub>3</sub> *	→	HCOOCH <sub>3</sub> * + H*	5.79x10 <sup>14</sup>	-	s <sup>-1</sup>	31.96	-	-
k <sub>9</sub>	HCOOCH <sub>3</sub> *	→	HCOOCH <sub>3</sub>	1.49x10 <sup>16</sup>	-	s <sup>-1</sup>	55.60	-	-

<sup>†</sup> Indicates sticking probability.

<sup>‡</sup> R<sup>2</sup> value from equilibrium constant k<sub>3a</sub>/k<sub>3b</sub>.

\* Assumed based on k<sub>4a</sub>

\*\* No experimental value is available, 5.00 was assumed to initiate the calculation.

### Transient pulse/response analysis

The kinetic analysis of micropulse reactors is well developed<sup>28–33</sup> and enables detailed modeling of the transient responses using the complex reaction network (Scheme 1). In brief, diffusion equations/reaction (including adsorption) were employed to describe the chemical reactions throughout the diffusion-mixed catalytic reactor, yielding the time dependent yield of each product (Supplementary VI). The appropriate rate expressions were used for the microkinetic representation for each elementary reaction step (Scheme 1). To obtain rate constants for each step using regression methods, initial values were taken from the single crystal surfaces (Table 1).

The extensive data from the transient responses (Figure 3, Table 1) provides ample information for testing the mechanism (Scheme 1) and refining the rate constants governing the catalytic cycle on the nanoporous gold.<sup>28,34</sup> The response of the reaction sequence (Scheme I) to the methanol pulses in the reactor was microkinetically modeled, both axially and time resolved, using a *finite*

*difference* method (Methods, Supplementary VI). The known oxygen coverage, methanol pulse size and the physical parameters of the reactor (see Supplementary VI) were included in the simulation. Initial values of the rate constants from the model studies were regressed at each temperature by fitting the simulated results to the experimental product selectivity (solid lines, Figure 2). Steps in the mechanism shown by sensitivity analysis<sup>35</sup> to have no effect on the product selectivity ( $k_6$ ,  $k_8$ , and  $k_9$ ), were fixed at their estimated values. For all points the fit was excellent ( $R^2$  value of 0.9999, Supplementary VII). Generally only small adjustments to the kinetic parameters measured on the single crystals were required to recreate the experimental results with very high precision (Table 1); these adjustments are generally within the experimental accuracy of the initial estimated values.

### **Connecting single crystal, pulse and catalytic reactions**

*First, the striking agreement between the rate constants shows that for oxygen-assisted methanol coupling there is no inherent material or temperature “gap” from the single crystal studies and the catalyst. It also underscores the advantage of time-resolved kinetic measurements under well-defined transport conditions, such as TAP, for obtaining accurate rate parameters at the microkinetic level of mechanistic detail.*

As noted briefly above, under catalytic (ambient) conditions over npAu and in the model studies on single crystal gold the selectivity for methyl formate formation is > 90%, far different from that observed under the Knudsen flow pulse conditions. Further, in the pulse experiments the pressure of methanol in the reactor reached only  $\sim 10^{-5}$  bar,<sup>33</sup> far below that used in the catalytic reactor (1 bar). *These differences can be readily reconciled based on the fundamental knowledge of the reaction mechanism (Figure 1 and Scheme 1) and the rate constants derived therefrom (Table 1).* A microkinetic model built from this information was used to predict the selectivity for a wide range of pressures and oxygen coverages and for temperatures of 383, 423 and 463 K, by increasing the methanol pulse size into the reactor in order to increase the methanol mean pressure (Supplementary VI), simulating a continuum of pressure from  $10^{-8}$  to  $10^2$  bar (Figure 5). The atomic oxygen coverage on the surface was also varied from  $10^{-5}$  to 1 monolayers. Contour plots show the selectivity for partial oxidation to methyl formate depends strongly on the methanol pressure, whereas the selectivity for formaldehyde vs.  $\text{CO}_2$  is more sensitive to the oxygen coverage (Figure 5). For a mean pressure of 1 bar at 423 K the coupling selectivity to methyl formate exceeds 95% for oxygen coverages above  $5 \times 10^{-4}$  ML. Further, lowering the reaction temperature shifts the selectivity toward the coupling product at lower reactant pressures, as observed in the pulsed flow Knudsen reactor (Figure 4).

*The kinetic model accurately predicts the high selectivity for methyl formate production (>98%) for conditions that best mimic the flow reactor (0.1 bar methanol mean pressure, 0.05 monolayers of oxygen, star on Figure 5), thus, validating the model and the approach. Similarly, high selectivity to methyl formate (>99%) was computed when the kinetic parameters were used in a plug flow simulation of 10% methanol in Ar mixture at 1 bar with a constant oxygen coverage of 0.05 monolayers (see Figure S5, Supplementary VIII). The model also accurately predicts the predominance of formaldehyde production observed in some of the transient conditions, e.g. at 463 K and  $10^{-5}$  bar (Figure 5, dashed lines), further validating the kinetic model.*

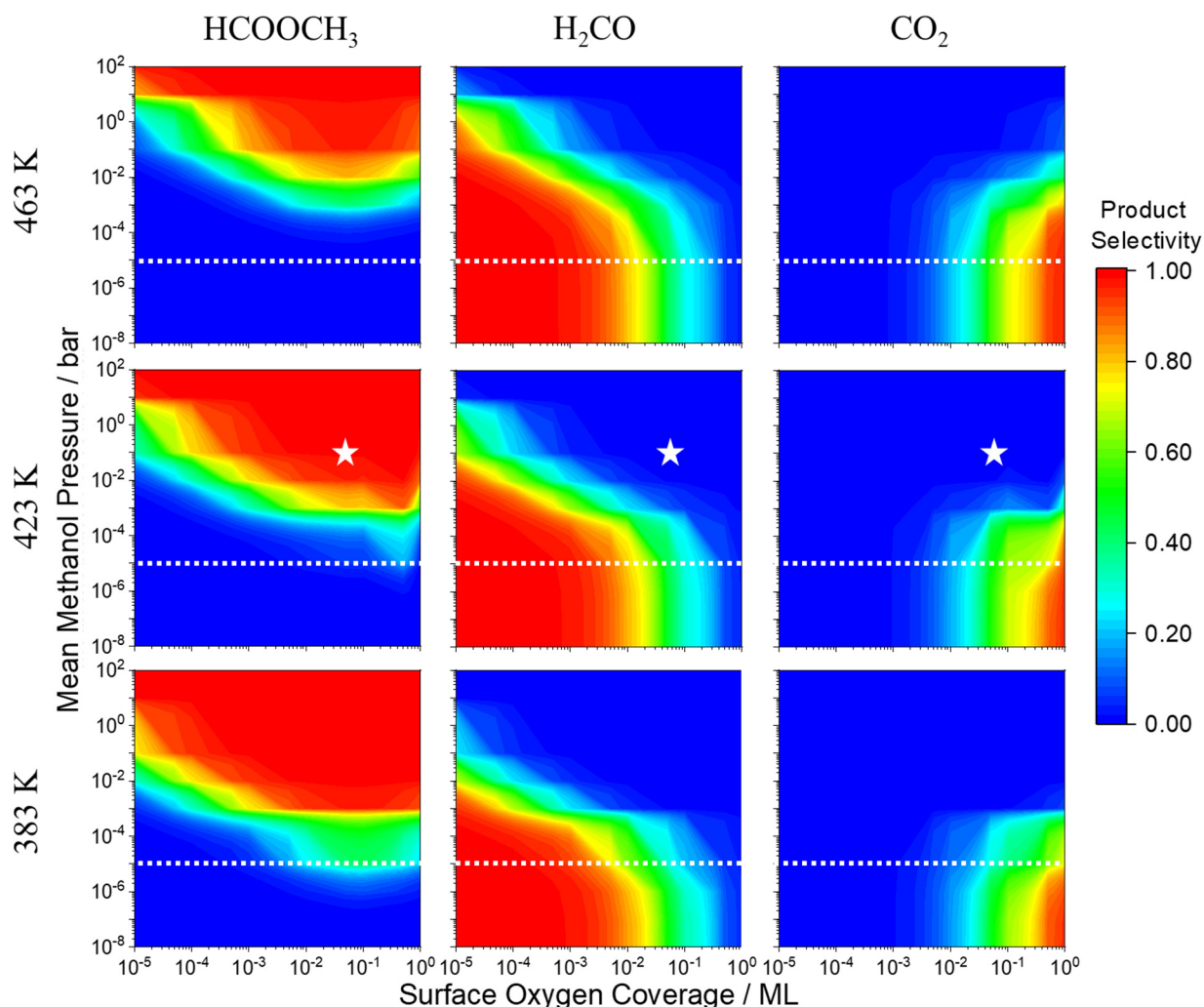


**Figure 5.** Computed product selectivity contours for methanol coupling over nanoporous  $\text{Ag}_{0.03}\text{Au}_{0.97}$  as a function of the effective methanol pressure in a pulse and the surface coverage of adsorbed oxygen at 383, 423, and 463 K. Under catalytic conditions the active sites are saturated with adsorbed O. The mean pressure during a standard pulse experiment is  $\sim 10^{-5}$  bar and is indicated by the white dashed line on the contour plots. *O* coverages were extended to 1.0 ML, though this concentration exceeds that expected for the catalyst surface (star.) The white star denotes conditions that replicate flow reactor experiments (0.1 bar mean methanol pressure, and 0.05 monolayers of  $\text{O}^*$  coverage, and the site concentration was determined by titration with  $\text{O}_2$  pulses).<sup>36</sup>

The simulations show explicitly that the large differences in selectivity patterns that are observed when comparing results from single crystal studies and the operational catalysts is a pressure *effect* rather than a pressure “gap” as it is often referred to in the literature. In other words, we demonstrate the fundamental kinetics and mechanism are continuous across pressure regimes, and the fundamental difference is the relative surface concentration of intermediates/reactants; there are **no** inherent differences in reaction mechanisms under the two conditions.

## The origin of the pressure and temperature effects

The high selectivity for methyl formate observed in both single-crystal and catalytic studies at atmospheric pressure is attributed to the dominance of methoxy on the surface. In the model studies methanol reacts nearly to completion with preadsorbed oxygen below 150 K to form adsorbed methoxy, with  $\beta$ -H elimination to yield formaldehyde ensuing at  $\sim 200$  K. Under these conditions the surface lifetime of formaldehyde is long and reaction with adsorbed methoxy to form the coupled intermediate (hemiacetal alcoholate) is facile. Furthermore, the concentration of adsorbed O is near zero, due to reaction with excess methanol at 135 K, so that formaldehyde cannot be further oxidized. Thus, without excess oxygen and with readily accessible methoxy, the conversion to methyl formate dominates.

The kinetics also drive the selectivity *via* the methoxy intermediate to methyl formate under catalytic conditions. Knowledge of the mechanism and the rate constants for each elementary step allows the surface concentration of each reactive intermediate to be calculated from the microkinetic model under all conditions studied. The effect of pressure is due to the change in the relative surface concentration of the intermediates under the different conditions. Of most significance is the fraction of adsorbed methoxy,  $F_{\text{CH}_3\text{O}^*}$

$$F_{[\text{CH}_3\text{O}^*]} = \frac{[\text{CH}_3\text{O}^*]}{[\text{CH}_3\text{O}^*] + [\text{CH}_2\text{O}^*] + [\text{H}_2\text{CO}_2^*]} \quad (1)$$

For typical reactor conditions of 423 K and a surface of O\* of 0.05 ML increasing the mean pressure of methanol from  $10^{-8}$  to  $10^2$  bar increases the fraction of methoxy sigmoidally, leading to complete dominance of methoxy above a mean methanol pressure of  $\sim 0.01$  bar (Figure 6). Accordingly, the selectivity to methyl formate exceeds 90% above a methoxy surface ratio of 0.6. This result is the consequence of the relative rates of the competing reactions. Under conditions of excess methoxy on the surface, whenever formaldehyde is formed the coupling pathway dominates; *i.e.*,

$$k_7[\text{CH}_3\text{O}^*][\text{CH}_2\text{O}^*] \gg k_{4a}[\text{O}^*][\text{CH}_2\text{O}^*] \geq k_{3a}[\text{CH}_2\text{O}^*] \quad (2)$$

The predominance of formaldehyde production in the transient experiments at 463 K is due to a low coverage of methoxy and the relatively short surface lifetime of formaldehyde in the catalytic flow conditions.

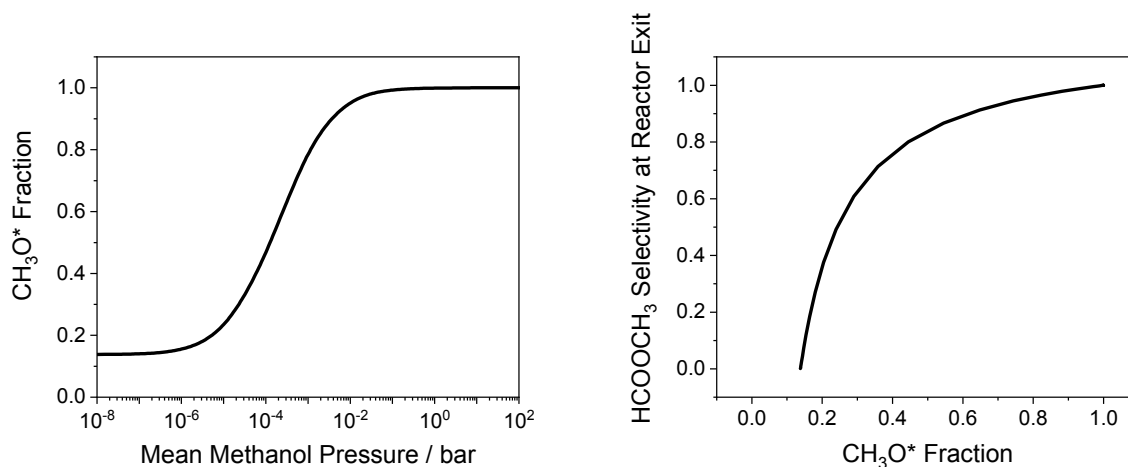


**Figure 6.** Left) The fraction surface-bound methoxy relative to all surface intermediates as a function of the mean methanol pressure in the reactor. Right) the selectivity to methyl formate ( $\text{HCOOCH}_3$ ) in the reactor exit as a function of the fractional of the surface bound intermediates that is  $\text{CH}_3\text{O}^*$ . From pulse experiment simulations at 423 K and an oxygen coverage of 0.05ML. Obtained from microkinetic modeling where the inlet pulse size is varied to yield a mean methanol pressure of  $10^{-10}$  to  $10^2$  bar in the reactor)

The successful modeling of catalytic behavior demonstrated here illustrates the potential for accurate and quantitative predictions for working catalytic systems based on reaction mechanisms and rate parameters derived from single-crystal studies. The success of this methodology for a complex reaction network depends on several key factors. Most importantly, the composition of the surface and the availability of active sites (herein  $\text{O}_{\text{ads}}$ ) should be similar in the different regimes. Gold is a particularly favourable case because the active site concentration can be tuned with metal additives. Hence, the generalization of this method to other oxidation reactions on the nanoporous  $\text{Ag}_{0.03}\text{Au}_{0.97}$  and to other binary alloys of gold or other noble metals is anticipated. Furthermore, these reactions exhibit little sensitivity to the structure of the gold surface, another important aspect of linking the reactivity across different states of the material. Lastly, the mechanism must be preserved throughout the range of P, T and material space. Generally, one would expect similar success with structure insensitive catalytic reactions on noble metal catalysts. Extension to structure sensitive reactions would require a more extensive set of kinetic studies on surfaces of varying structure.

## Conclusions

Fundamental mechanistic and kinetic information determined from single crystal studies in ultrahigh vacuum allows the prediction of the selectivity for oxygen-assisted esterification of methanol over nanoporous gold catalysts under practical catalytic conditions. Rate constants for elementary steps comprising the catalytic cycle obtained on gold single crystals in the temperature range from 150 – 200 K are consistent with those determined on the actual catalytic material at operational temperature (370 – 425 K) by transient -pressure-pulse-response method. Microkinetic analysis shows that the selectivity toward the ester is governed by the concentration of surface-bound methoxy, which dominates the adsorbed reaction intermediates above  $\sim 10^{-2}$  bar. Critical to this multidimensional scaling were both the single crystal and the pulse-response TAP

experiments, the latter providing the insight into the origin of the effects of (1) changing material state, (2) increasing temperature by 200 K and (3) increasing pressure over nine decades. This study shows the importance of fundamental kinetic studies for the understanding and prediction of heterogeneous catalytic performance and progress toward “catalysis by design.”

## Methods

### Synthesis and activation of the npAu material.

The npAu foil catalyst was synthesised according to the previous reported method.<sup>18</sup> Sheets of 6 karat white gold foils (85% Ag/15% Au) were chemically etched in 70% HNO<sub>3</sub> for 30 minutes. The dealloyed foils were then filtered using excess water over a quartz frit and dried at 323 K under He flow. The npAu foils were then activated in a flow reactor via a temperature ramp from 303 K to 423 K (10 K/min) in a flow of 60 g/Nm<sup>3</sup> of ozone in a ~50% O<sub>2</sub>/He gas mixture at a flow rate of 50mL/min at 1 atm and held for one hour. This was followed by exposure to a stream of 10% methanol and 20% O<sub>2</sub> in He at 1atm, ramping from 323 to 423 K until constant activity was seen. The activated catalyst was then transferred to the TAP reactor, the sample was then evacuated and reduced via sequential pulsing of methanol.

### Transient pulse-response Temporal Analysis of Products (TAP) experiments .

To mimic the state of the activated catalyst under flow conditions for the pulse measurements, the npAu was first oxidized using ozone and then partially reduced by CO. It is known that the CO removes the unselective gold oxide that forms initially in the activation procedure with ozone, and leaves behind the *selective oxygen* species that is involved in the partial oxidation of methanol to methyl formate.<sup>25</sup> The sample was housed in a quartz microreactor evacuated to 10<sup>-8</sup> torr as part of a commercial TAP-2 type reactor<sup>28</sup> which has both flow and pulse capabilities. During a pulse experiment the time resolved exit flow of gas is recorded via QMS at the reactor exit, the pulse responses are integrated, and the total gas composition calculated. Due to limitations of the QMS only one M/Z could be measured per pulse, therefore to scan all M/Z values multiple pulses are required. This combination of pulses will hereby be referred to as a *pulse set*. The quartz microreactor was packed in a *thin zone* configuration with a layer of ~350 micron SiC (20.1 mm) followed by a layer of npAu catalyst (2.1 mm) followed by a final layer of SiC (26.0 mm) for a total reactor length of 48.4 mm.

For the initial oxidation a mixture of ozone (60 g/Nm<sup>3</sup>) in oxygen was bled in to the reactor at a rate that sustained a pressure of ~2x10<sup>-6</sup> torr in the chamber for 40 minutes. The oxidized catalyst was then heated to 403 K and exposed to repeated pulses of a CO/Ar mixture at while measuring M/Z 28 and 44 (CO and CO<sub>2</sub> respectively) until CO<sub>2</sub> production had ceased. During the methanol pulse experiments nanomolar (~1x10<sup>14</sup> molecules) pulses of methanol in a methanol/Ar mixture were passed over the pre-reduced npAu catalyst at temperatures ranging from 363 to 423 K. 5 pulses were required to probe measured M/Z values 60, 44, 40, 31, and 30 relating to methyl formate, CO<sub>2</sub>, argon, methanol and formaldehyde respectively. During each pulse set surface oxygen is being consumed, therefore it is possible to probe a range of oxygen coverages through sequential pulsing. Pulse sizes were chose to ensure Knudsen flow throughout the reactor.

**Quantification of TAP pulse responses.** In order to calculate the selectivity of the products, total correction factors (TCFs) for determining the number density of molecules in the QMS ioniser were calculated using the equation derived in Xu *et al.*<sup>37</sup> This procedure allows quantification of the number of moles of products without having to calibrate each of the individual gases to the argon tracer. The total amount of gas in a TAP pulse is taken as the integral of the time resolved transient. To calculate the selectivity of the products, first the fragments for the various products are removed from the transient response (*e.g.* the M/Z 31 fragment from methyl formate was subtracted from the methanol transient), they are then correct using their respective TCF value. To calculate the composition of the gas mixture at the reactor exit, first the responses were corrected using the procedure outlined in Supplementary I-II. The pulses were then integrated with respect to time giving a total concentration detected at the reactor exit. Finally, the composition of the gas at the reactor exit was calculated using:

$$\text{Gas Composition} = \frac{[C_X]}{[CH_3OH] + [CO_2] + [CH_2O] + 2[HCOOCH_3]} \quad (18)$$

where  $[C_X]$  is the amount of carbon present in a gas X. For the sake of stoichiometry, the selectivities were calculated based on the total amount of carbon present in the molecule.

### **Temperature Programmed Reaction Spectroscopy (TPRS, TPD),**

The TPRS experiments were performed on Au(110) single-crystal under UHV conditions in a chamber with a base pressure of  $10^{-10}$  torr. The methanol oxidation experiments consisted of initial ozone exposure of the clean Au(110) surface at 300 K, followed by cooling of the sample to 120 K, before dosing methanol. The initial oxygen coverage was calibrated to be 0.05 ML and the amount of adsorbed methanol on the O/Au(110) interface was in great excess. After dosing methanol onto the oxygen pre-dosed surface, the single crystal was heated at a constant rate and all products evolving into the gas phase were quantified by a quadrupole mass spectrometer (QMS). Similarly, TPD experiments were performed by adsorption of formaldehyde or methyl formate on the atomically clean Au(110) surface at 120 K and subsequent annealing of the Au single crystal with a constant rate of 5K/sec, following the desorbing mass fragments with a QMS. Analysis of the surface after such treatment showed no residual species remaining on the surface.

### **Microkinetic Modeling**

In order to clarify our use of the term “microkinetic modeling” we offer the following definition, which is currently widely used in the literature<sup>35,38,39</sup>.

In **microkinetic** analysis all elementary steps comprising the reaction mechanism are considered explicitly, and no assumptions about the rate-determining step are made.

Implicit in this definition is the knowledge of the important elementary steps and their rate constants. In other words, the postulated mechanism may consist of as few or as many elementary steps at the discretion of the modeler. The corresponding kinetic model is considered “microkinetic”, as long as postulated (selected) steps and concentrations of surface intermediates are explicitly resolved. In the study reported here these facts were determined from single crystal

studies. The microkinetic analysis was performed on a surface with a specific O coverage, assumed constant. This assumption is consistent with reactor studies of methanol coupling on nanoporous gold catalysts which show saturation of the surface active sites by adsorbed O

**Data Analysis and Model Regression.** All post processing, data analysis, and model regressions were performed using the MATLAB (R2016b)<sup>40</sup> programming environment, using in-house purpose-built scripts.

### Data availability

The authors declare that the data supporting the findings of this study are available within the article and its Supplementary Information files, and all relevant data are available from the authors.

### References

1. Holdren, J. P. Materials genome initiative for global competitiveness. *Natl. Sci. Technol. Counc. OSTP. Washington, USA* (2011).
2. Hattrick-Simpers, J., Wen, C. & Lauterbach, J. The Materials Super Highway: Integrating High-Throughput Experimentation into Mapping the Catalysis Materials Genome. *Catal. Letters* **145**, 290–298 (2015).
3. Nørskov, J. K., Bligaard, T., Rossmeisl, J. & Christensen, C. H. Density functional theory in surface chemistry and catalysis. *Nat. Chem.* **1**, 37–46 (2009).
4. Nørskov, J. K., Abild-Pedersen, F., Studt, F. & Bligaard, T. Density functional theory in surface chemistry and catalysis. *Proc. Natl. Acad. Sci.* **108**, 937–943 (2011).
5. Xu, J. G. & Froment, G. F. Methane Steam Reforming, Methanation and Water-Gas Shift .1. Intrinsic Kinetics. *Aiche J.* **35**, 88–96 (1989).
6. Gleaves, J. T., Ebner, J. R. & Kuechler, T. C. Temporal Analysis of Products (TAP)—A Unique Catalyst Evaluation System with Submillisecond Time Resolution. *Catal. Rev.* **30**, 49–116 (1988).
7. Stahl, S. S. Palladium-catalyzed oxidation of organic chemicals with O<sub>2</sub>. *Science* **309**, 1824–1826 (2005).
8. Sheldon, R. A. Heterogeneous Catalytic Oxidation and Fine Chemicals. in *Heterogeneous Catalysis and Fine Chemicals II Proceedings of the 2nd International Symposium* **59**, 33–54 (1991).
9. Sheldon, R. A. Catalytic Oxidations in the Manufacture of Fine Chemicals. *Stud. Surf. Sci. Catal.* **55**, 1–32 (1990).
10. Xu, B. & Friend, C. M. Oxidative coupling of alcohols on gold: Insights from experiments and theory. *Faraday Discuss.* **152**, 307 (2011).
11. Stowers, K. J., Madix, R. J. & Friend, C. M. From model studies on Au(111) to working conditions with unsupported nanoporous gold catalysts: Oxygen-assisted coupling reactions. *J. Catal.* **308**, 131–141 (2013).
12. Xu, B., Haubrich, J., Baker, T. A., Kaxiras, E. & Friend, C. M. Theoretical study of O-assisted selective coupling of methanol on Au(111). *J. Phys. Chem. C* **115**, 3703–3708

- (2011).
13. Wachs, I. E. & Madix, R. J. The surface intermediate H<sub>2</sub>COO. *Appl. Surf. Sci.* **5**, 426–428 (1980).
  14. Outka, D. A. & Madix, R. J. Acid-base and nucleophilic chemistry of atomic oxygen on the Au(110) surface: Reactions with formic acid and formaldehyde. *Surf. Sci.* **179**, 361–376 (1987).
  15. Xu, B., Liu, X., Haubrich, J., Madix, R. J. & Friend, C. M. Selectivity control in gold-mediated esterification of methanol. *Angew. Chemie - Int. Ed.* **48**, 4206–4209 (2009).
  16. Xu, B., Madix, R. J. & Friend, C. M. Predicting gold-mediated catalytic oxidative-coupling reactions from single crystal studies. *Acc. Chem. Res.* **47**, 761–772 (2014).
  17. Sexton, B. A. & Madix, R. J. A vibrational study of formic acid interaction with clean and oxygen-covered silver (110) surfaces. *Surf. Sci.* **105**, 177–195 (1981).
  18. Personick, M. L. *et al.* Ozone-Activated Nanoporous Gold: A Stable and Storable Material for Catalytic Oxidation. *ACS Catal.* **5**, 4237–4241 (2015).
  19. Sault, A. G., Madix, R. J. & Campbell, C. T. Adsorption of oxygen and hydrogen on Au(110)-(1x2). *Surf. Sci.* **169**, 347–356 (1986).
  20. Meyer, R., Lemire, C., Shaikhutdinov, S. K. & Freund, H.-J. Surface chemistry of catalysis by gold. *Gold Bull.* **37**, 72–124 (2004).
  21. Wittstock, A. *et al.* Nanoporous Au: An unsupported pure gold catalyst? *J. Phys. Chem. C* **113**, 5593–5600 (2009).
  22. Wittstock, A. *et al.* Nanoporous gold catalysts for selective gas-phase oxidative coupling of methanol at low temperature. *Science* **327**, 319–22 (2010).
  23. Getman, R. B., Xu, Y. & Schneider, W. F. Thermodynamics of environment-dependent oxygen chemisorption on Pt(111). *J. Phys. Chem. C* (2008). doi:10.1021/jp800905a
  24. Mulla, S. S., Chen, N., Delgass, W. N., Epling, W. S. & Ribeiro, F. H. NO<sub>2</sub> inhibits the catalytic reaction of NO and O<sub>2</sub> over Pt. *Catal. Letters* (2005). doi:10.1007/s10562-004-3466-1
  25. Zugic, B. *et al.* Dynamic restructuring drives catalytic activity on nanoporous gold–silver alloy catalysts. *Nat. Mater.* **16**, 558–564 (2016).
  26. Redhead, P. A. Thermal desorption of gases. *Vacuum* **12**, 203–211 (1962).
  27. Falconer, J. L. & Madix, R. J. Flash desorption activation energies: DCOOH decomposition and CO desorption from Ni (110). *Surf. Sci.* **48**, 393–405 (1975).
  28. Gleaves, J. J. T., Yablonskii, G. G. S., Phanawadee, P. & Schuurman, Y. *TAP-2: An interrogative kinetics approach. Applied Catalysis A: General* **160**, 55–88 (1997).
  29. Shekhtman, S. O., Yablonsky, G. S., Chen, S. & Gleaves, J. T. Thin-zone TAP-reactor--theory and application. *Chem. Eng. Sci.* **54**, 4371–4378 (1999).
  30. Shekhtman, S. O., Yablonsky, G. S., Gleaves, J. T. & Fushimi, R. R. Thin-zone TAP reactor as a basis of ‘state-by-state transient screening’. *Chem. Eng. Sci.* **59**, 5493–5500 (2004).
  31. Yablonsky, G. S., Olea, M. & Marin, G. B. Temporal analysis of products: basic principles, applications, and theory. *J. Catal.* **216**, 120–134 (2003).
  32. Shekhtman, S. O., Yablonsky, G. S., Gleaves, J. T. & Fushimi, R. ‘State defining’ experiment in chemical kinetics - Primary characterization of catalyst activity in a TAP experiment. *Chem. Eng. Sci.* **58**, 4843–4859 (2003).
  33. Gleaves, J. T., Yablonsky, G., Zheng, X., Fushimi, R. & Mills, P. L. Temporal analysis of products (TAP)—recent advances in technology for kinetic analysis of multi-component

- catalysts. *J. Mol. Catal. A Chem.* **315**, 108–134 (2010).
34. Constales, D., Yablonsky, G. S., Marin, G. B. & Gleaves, J. T. Multi-zone TAP-reactors theory and application: I. The global transfer matrix equation. *Chem. Eng. Sci.* **56**, 133–149 (2001).
  35. Campbell, C. T. The Degree of Rate Control: A Powerful Tool for Catalysis Research. *ACS Catalysis* **7**, 2770–2779 (2017).
  36. Wang, L.-C. *et al.* Active sites for methanol partial oxidation on nanoporous gold catalysts. *J. Catal.* **344**, Ahead of Print (2016).
  37. Xu, B., Madix, R. J. & Friend, C. M. Achieving optimum selectivity in oxygen assisted alcohol cross-coupling on gold. *J. Am. Chem. Soc.* **132**, 16571–16580 (2010).
  38. Stoltze, P. Microkinetic simulation of catalytic reactions. *Prog. Surf. Sci.* **65**, 65–150 (2000).
  39. Saliccioli, M., Stamatakis, M., Caratzoulas, S. & Vlachos, D. G. A review of multiscale modeling of metal-catalyzed reactions: Mechanism development for complexity and emergent behavior. *Chem. Eng. Sci.* **66**, 4319–4355 (2011).
  40. The Mathworks Inc. MATLAB - MathWorks. [www.mathworks.com/products/matlab](http://www.mathworks.com/products/matlab) (2016). Available at: <http://www.mathworks.com/products/matlab/>.

## Acknowledgements

This work was supported as part of the Integrated Mesoscale Architectures for Sustainable Catalysis (IMASC), an Energy Frontier Research Center funded by the U.S. Department of Energy (DOE), Office of Science, Basic Energy Sciences (BES), under Award number DE-SC0012573. E.R. expresses his gratitude to Prof. Unni Olsbye for her support and enthusiasm about applying TAP for mechanistic research in catalysis. E.R. acknowledges the Norwegian Research Council for financial support through contract 239193.

## Author contributions

R.J.M. and E.R. guided the research. C.R. and S.K. performed the experiments. C.R. performed the microkinetic modeling. All authors contributed significantly to writing the manuscript.

## Additional information

Supplementary information accompanies this paper.

## Competing financial interests

The authors declare no competing financial interests.